Anisoplanatism in Adaptive Optics Compensation of a Focused Beam Using Distributed Beacons

Phillip D. Stroud
LAUR 92-479
Los Alamos National Laboratory, MS-F607, Los Alamos, NM 87544

Journal of the Optical Society of America A Vol. 13, No 4, pp 868-874, April 1996.

ABSTRACT

In systems that achieve laser beam propagation through atmospheric turbulence by phase compensation with adaptive optics, the performance depends on the beacon's spatial distribution. A formulation is obtained to calculate the anisoplanatic Strehl ratio of a phase compensated, focused beam for any beacon distribution and turbulence profile. Analytic results are obtained for several beacon geometries corresponding to practical systems, in the large aperture limit. The effects of finite aperture are evaluated for two representative beacon geometries, using both uniform and highly localized turbulence profiles. The spread of the beacon distribution is found to be much less deleterious than the offset of the beacon centroid from the aimpoint. The anisoplanatic effect is qualitatively different in systems characterized by a focused beam geometry and systems where the collimated beam geometry applies.

INTRODUCTION

Index of refraction fluctuations associated with atmospheric turbulence can catastrophically degrade the propagation of an image or a laser beam through the atmosphere. In many systems of interest, much of this degradation can be compensated by the use of an adaptive optics system that corrects the optical phase profile of the outgoing laser beam to cancel the effect of the turbulence. The adaptive optics system obtains the required phase correction by detecting a beacon signal, which is generated in such a place that it traverses the same regions as the light being compensated. Practically, however, there will be some error in the phase correction, because the beacon light does not travel the exact path of the light being compensated. This error, due to partially correlated differences in the refraction index perturbations sampled by the beacon and the beam, produces what are known as anisoplanatic effects, which reduce the performance of the adaptive optics system from ideal.

The many applications for adaptive optics compensation can be categorized by geometry, and each geometry has an associated set of anisoplanatic problems. For terrestrial based imaging of astronomical objects, effective beacons can be provided by a bright star[1], an artificial laser star[2], or Rayleigh backscatter[3]. For imaging of (or laser propagation to) an orbiting object, a beacon can also be provided by light generated on or reflected from the object, or a co-orbiting object[4]. For imaging of or laser propagation to a relatively slow moving object such as an airplane or theater missile, a lead ahead beacon can be provided by reflecting light from a target

region ahead of the aimpoint, such that the aimpoint moves to the beacon region in the time needed for light to make a round trip.

In geometries where an aperture is focused on some object and a point source beacon is located at the same focal distance, a major source of anisoplanatic degradation is angular displacement (the difference in directions between the beacon and the imaging or aim point). This anisoplanatic degradation was characterized by Fried[5] and by Sasiela[6]. Yura[7] and Sasiela[8] also obtained formulations for the focal plane intensity profile obtainable with an adaptive optics system using an offset point beacon located at the focal distance. This geometry applies to a bright star beacon for astronomical imaging, and to an orbiting object that is used to reflect a beacon for itself (the angular offset in this case is the roughly 50 microradians that a low earth orbit satellite subtends in the light round-trip time.)

In geometries where an aperture is focused to an infinite focal length and a point source beacon is in the same direction that the aperture is pointing, but at a finite distance, a major anisoplanatic effect comes from the difference between the collimated beam and the spherical wave beacon. The nature of this so called focus anisoplanatism has been analyzed and characterized for several turbulence models and beacon altitudes, by Tyler[9], Fried & Belsher[10], and Welsh & Gardner[11]. This geometry describes an on-axis laser generated point beacon for astronomical imaging.

In geometries where an aperture is focused at some arbitrary distance, and a point beacon source is located at a different distance and in a slightly different direction, there is a combination of angular and focal anisoplanatism. Formulations for the beam degradation to be expected in this case have been developed by Tyler[12] and by Stone et.al.[13] and applied in the limit of an infinite focal length. This geometry describes an off-axis laser generated point beacon for astronomical imaging. Sasiela[8,14] developed a formulation for finding the anisoplanatic effect with a distributed beacon, and characterized the case of a uniform circular beacon source with a collimated beam.

In this paper, a formulation is developed for the geometry where an aperture is focused on some object at finite distance, and a beacon is located at the same focal distance, but the beacon is distributed about some centroid, and this centroid is offset from the aimpoint. An anisoplanatic effect arises from the finite size of the beacon, and the offset of the beacon centroid from the aimpoint. This geometry applies, for example, when an illuminator laser is used to generate the beacon by lighting up part of the object of interest. The beacon will have some distribution in the target plane, determined by the diffraction of the illuminator laser, the steering, scattering and scintillation of the illuminator light by the atmosphere, the illuminator pointing error, and the motion, shape, size and reflectivity of the target. This analysis characterizes the anisoplanatic effect when an offset distributed beacon is used to compensate a focused beam. The effect is examined for various beacon distributions. In addition, the dependence on the aperture size and on the turbulence profile is examined.

FORMULATION OF ANISOPLANATIC STREHL RATIO

The geometry for a focused beam using a distributed beacon is shown in Fig. 1. The z axis has its origin at the center of the aperture, and points to the aimpoint. The telescope aperture radius is R (diameter is D), and the focal length is L. A point in space is specified by a 2D radial vector, $\vec{\rho}$, and its distance along the optical axis, z. The instantaneous index of refraction perturbation due to turbulence, at a position ($\vec{\rho}$, z) is written n[$\vec{\rho}$, z]. For any point on the aperture, the residual phase error is the phase perturbation due to turbulence for propagation from that aperture point to the aimpoint, minus the phase correction applied at that aperture point. The

2

phase perturbation due to turbulence for propagation from aperture point A at position $(\vec{\rho}_A, 0)$ to the aimpoint, is obtained from the perturbation in the optical path length[15] between the two points:

$$\phi_{A,beam} = k_0 \int_0^L dz\; n\left[\hat{\gamma}\vec{\rho}_A, z\right] \tag{1}$$

where $k_0 = 2\pi/\lambda$ is the wavenumber of the light, $\gamma \equiv z / L$ and $\hat{\gamma} \equiv 1 - z / L$. This formulation does not treat amplitude perturbations or diffraction.

The phase correction applied at any aperture point is determined by the average over the distributed beacon, of the phase perturbations sensed in the incoming beacon light. This assumes that the distributed beacon is an incoherent light source. A radial position in the target plane is represented by $\vec{b}$, and the normalized strength of the distributed beacon at radial position $\vec{b}$ is written $B(\vec{b})$, where the integral of $B(\vec{b})$ over all $\vec{b}$ is unity. The phase correction that is applied at aperture position $\vec{\rho}_A$ is

$$\phi_{A,beacon} = k_0 \int d^2\vec{b}\, B(\vec{b}) \int_0^L dz\; n\left[\hat{\gamma}\vec{\rho}_A + \gamma\vec{b}, z\right] \tag{2}$$

The residual phase error at aperture point A is thus

$$\phi_A = k_0 \int d^2\vec{b}\, B(\vec{b}) \int_0^L dz \left(n\left[\hat{\gamma}\vec{\rho}_A, z\right] - n\left[\hat{\gamma}\vec{\rho}_A + \gamma\vec{b}, z\right] \right) \tag{3}$$

Additional degradation caused by imperfect application of the sensed phase correction is not treated here. The beacon is presumably strong enough that statistical sampling noise is negligible.

The impact of the anisoplanatic error can be characterized by a reduction in deliverable aimpoint intensity from that obtainable in the absence of turbulence. This ratio of intensities with and without the anisoplanatic effect, known as the Strehl ratio, S, can be obtained from the residual phase errors with[16]

$$S = \int_A \int_B \exp\left(-\tfrac{1}{2} \left\langle \left(\phi_A - \phi_B \right)^2 \right\rangle \right) \tag{4}$$

where $\int_A \bullet \equiv \left(1/\pi R^2\right) \int\limits_{aperture} d^2\vec{\rho}_A \bullet$ is a shorthand notation for an aperture average. The angle brackets denote an ensemble average over different realizations of the refractive index fluctuations. The mutual coherence function of the residual aperture phase, defined as $M(\vec{\rho}_A, \vec{\rho}_B) \equiv \exp\left(-\tfrac{1}{2} \left\langle \left(\phi_A - \phi_B \right)^2 \right\rangle \right)$, is used here only to obtain a Strehl ratio, but it can be used to obtain other measures of the performance of an optical compensation system[17,18]. When the Strehl ratio is over about 30%, the aperture averaging can be moved[15] inside the exponential to get an approximation to the Strehl ratio: $S \cong \exp\left(-\tfrac{1}{2} \int_A \int_B \left\langle \left(\phi_A - \phi_B \right)^2 \right\rangle \right)$. The structure function of the residual aperture phase, $D(\vec{\rho}_A, \vec{\rho}_B) \equiv \left\langle \left(\phi_A - \phi_B \right)^2 \right\rangle$ has also been used extensively in the literature in analyses of the performance of optical systems. A quantity called the effective phase variance, defined as

3

$$\sigma^2_{\phi,eff} \equiv \tfrac{1}{2}\int_A \int_B \left\langle \left(\phi_A - \phi_B\right)^2 \right\rangle \tag{5}$$

can be used as a measure of the anisoplanatic effect[19]. In terms of this effective phase variance, the Strehl ratio is approximately $S = \exp\left(-\sigma^2_{\phi,eff}\right)$.

The variance of the residual phase error at aperture position $\vec{\rho}_A$ is $\sigma^2_{\phi,A} \equiv \left\langle {\phi_A}^2 \right\rangle$. The aperture average of the variance of the residual phase error, $\sigma^2_{\phi,\infty} \equiv \int_A \left\langle {\phi_A}^2 \right\rangle$, is also known as the mean square wave-front distortion[12]. The Zernike piston component of any aperture function is its aperture average[20], so the aperture averaged variance of the residual phase error with its piston component removed is $\sigma^2_{\phi,eff} \equiv \int_A \left\langle \left(\phi_A - \int_B \phi_B\right)^2 \right\rangle$, which is exactly equivalent to the effective phase variance as defined in Eq. (5). A third completely equivalent expression for the effective phase variance is $\sigma^2_{\phi,eff} \equiv \int_A \left\langle \phi_A^2 \right\rangle - \int_A \int_B \left\langle \phi_A \phi_B \right\rangle$, where the first term is the mean square wave-front distortion, and the second term removes the piston component.

To find the effective phase variance, the residual phase errors at aperture points A and B from Eq. (3) are substituted into Eq. (5), giving

$$\sigma^2_{\phi,eff} \equiv \tfrac{1}{2}\int_A \int_B \left\langle \left(k_0 \int d^2\vec{b} B(\vec{b}) \int_0^L dz \left(n\left[\hat{\gamma}\vec{\rho}_A, z\right] - n\left[\hat{\gamma}\vec{\rho}_A + \gamma\vec{b}, z\right] - n\left[\hat{\gamma}\vec{\rho}_B, z\right] + n\left[\hat{\gamma}\vec{\rho}_B + \gamma\vec{b}, z\right]\right)\right)^2 \right\rangle$$

After the square is performed, the effective phase variance is the sum of 16 terms, each having the form $\tfrac{1}{2}k_o^2 \int_A \int_B \int d^2\vec{b} B(\vec{b}) \int d^2\vec{b}\,' B(\vec{b}\,') \int_0^L dz \int_0^L dz' \left\langle n\left[\vec{r}_1(z;\vec{b}), z\right] n\left[\vec{r}_2(z';\vec{b}\,'), z'\right] \right\rangle$, where $\vec{r}_1$ represents the radial position along either the beam or beacon ray from either point A or B in the aperture, and $\vec{r}_2$ represents any of these four in the primed set used to perform the square. Because of the interchangability of the A and B aperture averages, and the primed and unprimed integrations, the sixteen terms can be combined into six terms, of which three are simplified cases of the other three:

$$\sigma^2_{\phi,eff} = k_o^2 \int_A \int_B \int d^2\vec{b} B(\vec{b}) \int d^2\vec{b}\,' B(\vec{b}\,') \int_0^L dz \int_0^L dz' \left\langle \begin{array}{l} n\left[\hat{\gamma}\vec{\rho}_A, z\right] n\left[\hat{\gamma}'\vec{\rho}_A, z'\right] \\ -n\left[\hat{\gamma}\vec{\rho}_A, z\right] n\left[\hat{\gamma}'\vec{\rho}_B, z'\right] \\ -2n\left[\hat{\gamma}\vec{\rho}_A + \gamma\vec{b}, z\right] n\left[\hat{\gamma}'\vec{\rho}_A, z'\right] \\ +2n\left[\hat{\gamma}\vec{\rho}_A + \gamma\vec{b}, z\right] n\left[\hat{\gamma}'\vec{\rho}_B, z'\right] \\ +n\left[\hat{\gamma}\vec{\rho}_A + \gamma\vec{b}, z\right] n\left[\hat{\gamma}'\vec{\rho}_A + \gamma'\vec{b}\,', z'\right] \\ -n\left[\hat{\gamma}\vec{\rho}_A + \gamma\vec{b}, z\right] n\left[\hat{\gamma}'\vec{\rho}_A + \gamma'\vec{b}\,', z'\right] \end{array} \right\rangle \tag{6}$$

The correlation function for the refractive index fluctuations at two positions was given by Tatarski[21] as an integral over the Kolmogorov turbulence spectrum

$$\left\langle n\left[\vec{r}_1(z), z\right] n\left[\vec{r}_2(z'), z'\right] \right\rangle = 0.2073 C_n^2(z) \int d^2\vec{k} \int dk_z \frac{\exp\left(i\vec{k} \cdot \left(\vec{r}_1(z) - \vec{r}_2(z')\right) + ik_z(z - z')\right)}{\left(\vec{k}^2 + k_z^2\right)^{11/6}} \tag{7}$$

4

The turbulence strength is characterized by C_n^2(z), the Kolmogorov turbulence structure coefficient. The turbulence fluctuations have been expanded into Fourier components, where k_z represents the component in the z direction, and $\vec{k}$ represents the 2D components transverse to the z direction. A handy gimmick for performing two of the integrations (over z' and k_z) can be obtained with the Fourier transform[23] $\int_{-\infty}^{\infty} dx \int_{-\infty}^{\infty} dk f(k) \exp(ikx) = 2\pi f(k)\delta(k)$ (noting that practically all the contribution from the z' integral comes in the region near z, and using the symmetry of the correlation function):

$$\int dz' \left\langle n[\vec{r}_1(z), z]\, n[\vec{r}_2(z'), z'] \right\rangle = 0.2073 C_n^2(z) \int \frac{d^2\vec{k}}{k^{11/3}} \cos\left(\vec{k} \cdot (\vec{r}_1(z) - \vec{r}_2(z))\right) \tag{8}$$

Applying Eqs. (7) and (8) in Eq. (6), and rearranging with trig identities gives the effective phase variance to be

$$\sigma_{\phi,eff}^2 = 0.2073 k_o^2 L \int_0^1 d\gamma C_n^2(\gamma L) \int \frac{d^2\vec{k}}{k^{11/3}} \left[1 - \int_A \int_B \cos(\vec{k} \cdot (\vec{\rho}_A - \vec{\rho}_B)\hat{\gamma})\right] \left|1 - \int d^2\vec{b} B(\vec{b}) \exp(i\vec{k} \cdot \vec{b}\gamma)\right|^2 \tag{9}$$

The effect of the beacon anisoplanatism can be separated into a filter function

$$\begin{aligned} F(\vec{k}, \gamma) &= \left|1 - \int d^2\vec{b} B(\vec{b}) \exp(i\vec{k} \cdot \vec{b}\gamma)\right|^2 \\ &= \left[\int d^2\vec{b} B(\vec{b}) \left(1 - \cos(\vec{k} \cdot \vec{b}\gamma)\right)\right]^2 + \left[\int d^2\vec{b} B(\vec{b}) \sin(\vec{k} \cdot \vec{b}\gamma)\right]^2 \end{aligned} \tag{10}$$

and the aperture averages can be performed to give

$$\sigma_{\phi,eff}^2 = 0.2073 k_o^2 L \int_0^1 d\gamma C_n^2(\gamma L) \int d^2\vec{k} k^{-11/3} \left[1 - \Lambda_1^2(kR\hat{\gamma})\right] F(\vec{k}, \gamma) \tag{11}$$

where $\Lambda_1(x) \equiv 2J_1(x)/x$ is the Jahnke notation[22] for twice the first Bessel function divided by its argument.

Sasiela[14] obtained a formulation for the aperture average of the residual phase variance with some or none of the Zernike modes removed. His formulation has greater scope than Eq. (6) in that it includes diffraction, treats alternative geometries implicitly, and provides for removal of tilt as well as piston Zernike modes. He evaluated the case of a collimated beam and a distributed beacon at a finite distance, neglecting diffraction, and the effective phase variance for that case, obtained by combining Eqs. (10,19, 26 and 27) of his paper can be written

$$\sigma_{\phi,eff}^2 = 0.2073 k_o^2 L \int_0^1 d\gamma C_n^2(\gamma L) \int d^2\vec{k} k^{-11/3} \left[\int_A \left|1 - \exp(-i\vec{k} \cdot \vec{\rho}_A \gamma) \int d^2\vec{b} B(\vec{b}) \exp(i\vec{k} \cdot \vec{b}\gamma)\right|^2 - \left|\Lambda_1(kR) - \Lambda_1(kR\hat{\gamma}) \int d^2\vec{b} B(\vec{b}) \exp(i\vec{k} \cdot \vec{b}\gamma)\right|^2 \right]$$

In the collimated geometry, the aperture averaging can not be untangled from the beacon distribution averaging, as it can in the focused beam geometry. For a focused beam, a careful application of Sasiela's formulation[14] can lead to Eqs. (10) and (11).

5

If no phase correction was applied to the beam, the resulting filter function would be F(**k**)=1. Using this filter, and the integral $\int_0^\infty dx\, x^{-8/3}(1-\Lambda_1^2(x)) = 1.06498$, the effective phase variance obtained from Eq. (11) matches Fried's well-known result[5], giving $\sigma^2_{\phi,eff} = 1.033(D/r_0)^{5/3}$, where r_0 is the atmospheric coherence length for the path from 0 to L, defined by $r_o^{-5/3} = 0.4235k_o^2\int_0^L dzC_n^2(z)\hat{\gamma}^{5/3}$.

WAVE-FRONT DISTORTION WITH DISTRIBUTED BEACONS

As pointed out by Sasiela[14], in many cases of interest the mean square wave-front distortion (which includes the piston Zernike mode) provides a good approximation to the effective phase variance. The mean square wave-front distortion, obtained by a derivation analogous to that leading to Eq. (11), is found to be

$$\sigma^2_{\phi,\infty} = 0.2073k_o^2L\int_0^1 d\gamma C_n^2(\gamma L)\int d^2\vec{k}k^{-11/3}F(\vec{k},\gamma) \tag{12}$$

In the limit of large aperture, the piston component of the residual phase will tend to zero. The mean square wave-front distortion of Eq. (12) can therefore be interpreted as the effective phase variance in the large aperture limit. Even though Eq. (12) gives a smaller Strehl ratio than a finite aperture would really have, it can be used for a first comparison of anisoplanatic effects for various beacon geometries.

Offset Point Beacon

For a point beacon source, displaced from the aimpoint by $\mathbf{b}_o$, the beacon distribution, in terms of the Dirac delta function, is $B(\mathbf{b})=\delta(\mathbf{b}-\mathbf{b}_o)$. When this beacon distribution is substituted into Eq. (10), the integration over $\vec{b}$ is trivial, and the filter function is easily found to be

$$F(\vec{k},\gamma) = 2\left(1-\cos(\vec{k}\cdot\vec{b}_o\gamma)\right) \tag{13}$$

Using this filter, and the integral $\int_0^\infty dx\, x^{-8/3}2(1-J_0(x)) = 2.23666$, the phase variance obtained from Eq.(12) matches Fried's standard result[1]

$$\sigma^2_{\phi,\infty,Point} = (b_0/L\theta_0)^{5/3} \tag{14}$$

where θ_o is the isoplanatic patch angle[1], defined by $\theta_o^{-5/3} = 2.914k_o^2\int_0^L dzC_n^2(z)z^{5/3}$.

On-axis uniform circular beacon

For a uniform circular beacon source distribution, of radius R_b, centered at the aimpoint, the filter function from Eq. (10) is found to be[22]

$$F(\vec{k},\gamma) = \left[1-\Lambda_1(kR_b\gamma)\right]^2 \tag{15}$$

6

Using this filter, and the integral $\int_0^\infty dx\ x^{-8/3}(1-\Lambda_1(x))^2 = 0.155019$, the phase variance obtained from Eq.(12) is

$$\sigma^2_{\phi,\infty,Circle} = (0.2016 R_b / L\theta_0)^{5/3} \tag{16}$$

The phase variance from a circular beacon of radius R_b will thus be equivalent to the phase variance that would be obtained by a point beacon offset from the aimpoint by 0.2016 R_b. The path integral over the weighted turbulence profile is collected into the same isoplanatic patch factor as in the offset point case.

For an on-axis uniform circular beacon, in collimated beam geometry, Sasiela[14] obtained $F(\vec{k},\gamma) = 1 - 2\Lambda_1(kR_b\gamma)\Lambda_1(kR\gamma) + \Lambda_1^2(kR_b\gamma)$ as the filter function for finding the mean square wave-front distortion. In the limit that the beacon radius is much greater than the aperture radius, the phase variance obtained with this collimated geometry filter is identical to that given by Eq. (16) for the focused beam geometry (the kRγ argument of the second term can be replaced by 0 for the integrations of Eq. (12) in this limit). However, for the small beacon radius limit, the results are qualitatively different. An on-axis point beacon gives no anisoplanatic error in the focused beam geometry, but in the collimated geometry, there is a "focal" anisoplanatic effect due to the mismatch between the conical shaped beacon and the cylindrical shaped beam.

Offset uniform circular beacon

For an offset uniform circular beacon of radius R_b, offset from the aimpoint by a displacement **d**, the filter function is found to be

$$F(\vec{k},\gamma) = 1 - 2\Lambda_1(kR_b\gamma)\cos(\vec{k}\cdot\vec{d}\gamma) + \Lambda_1^2(kR_b\gamma) \tag{17}$$

Using this filter, the phase variance obtained from Eq.(10) is

$$\sigma^2_{\phi,\infty,OffsetCircle} = (0.2016 R_b / L\theta_0)^{5/3} K(d / R_b) \tag{18}$$

where K(e) is an auxiliary function defined in this geometry by

$$K(e) = 6.45082 \int_0^\infty dx\ x^{-8/3}(1 - 2J_0(xe)\Lambda_1(x) + \Lambda_1^2(x))^2 \tag{19}$$

For a beacon of radius R_b, $K(d/R_b)$ is the ratio of the phase variance with a beacon offset of d, to the phase variance with zero offset. For small values of d/R_b, K has an asymptotic value of unity. For large values of d/R_b, $K=(0.2016 d/R_b)^{-5/3}$, which with Eq.(18) gives the same phase variance as an offset point beacon. A numerical evaluation of this phase variance multiplier due to beacon offset is shown in Fig. 2.

For an offset uniform circular beacon, in collimated beam geometry, Sasiela[14] obtained $F(\vec{k},\gamma) = 1 - 2\Lambda_1(kR_b\gamma)\Lambda_1(kR\gamma)J_0(\vec{k}\cdot\vec{d}\gamma) + \Lambda_1^2(kR_b\gamma)$ as the filter function for finding the phase variance including piston.

If the offset to the center of a uniform circular beacon is fixed, the phase variance can be treated as a function of the beacon radius. The anisoplanatic phase variance is then found to be minimized when the beacon radius is 1.59 times the offset, in which case, the phase variance is reduced by a factor of 0.8527 from the value obtained with a point beacon at an offset of d.

7

Other beacon source distributions

For a Gaussian circular beacon source distribution given by a standard 2D Gaussian distribution $B(\vec{b}) = (2\pi\Sigma^2)^{-1}\exp\left(-b^2/(2\Sigma^2)\right)$, the filter function of Eq. (10) is found to be[23] $F(\vec{k},\gamma) = \left(1-\exp(-\Sigma^2 k^2\gamma^2/2)\right)^2$. Using this filter, and the integral $\int_0^\infty dx\, x^{-8/3}(1-\exp(-x^2/2))^2 = 0.408984$, the phase variance obtained from Eq.(7) is $\sigma_\phi^2 = (0.3611\,\Sigma/L\theta_0)^{5/3}$. In this limit of large aperture, the anisoplanatic phase variance from a Gaussian circular beacon of rms radius Σ will thus be equivalent to the phase variance that would be obtained by a point beacon with an offset of 0.3611Σ.

In a two point straddle beacon geometry, the beacon is composed of two point sources which straddle the aimpoint. The two points are located at positions $\mathbf{b}_o$ and -$\mathbf{b}_o$, in the target plane. The filter function is found to be $F(\vec{k}) = \left(1-\cos(\vec{k}\cdot\vec{b}_o z/L)\right)^2$. Using this filter, and the integral $\int_0^\infty dx\, x^{-8/3}(2(1-J_0(x))-(1-J_0(2x))/2)^2 = 0.4617$, the phase variance obtained from Eq.(7) is $\sigma_\phi^2 = (0.388\,b_0/L\theta_0)^{5/3}$.

In a circular ring beacon geometry, centered on the aimpoint, where the radius of the ring is $\mathbf{b}_o$, the filter function is given by $F(\vec{k},\gamma) = \left(1-J_0(kb_o\gamma)\right)^2$, and the resulting phase variance, including piston, is $\sigma^2_{\phi,\infty,Ring} = (0.3201\,b_0/L\theta_0)^{5/3}$.

For the geometry where the beacon source distribution is a uniform centered line segment with half length b_o in the target plane, centered at the aimpoint, the filter function is $F(\vec{k},\gamma) = \left(1-\sin(\vec{k}\cdot\vec{b}_o\gamma)/(\vec{k}\cdot\vec{b}_o\gamma)\right)^2$ and the resulting phase variance, including piston, is found to be $\sigma^2_{\phi,\infty,Line} = (0.1663\,b_0/L\theta_0)^{5/3}$.

EFFECTIVE PHASE VARIANCE WITH DISTRIBUTED BEACONS

The effective phase variance, for an arbitrary aperture size, can be found by putting the various anisoplanatic filters into Eq. (11). The effective phase variance will depend on the turbulence profile in a more complicated way than can be incorporated into the isoplanatic patch angle. The effective phase variance can be cast as the product of the mean square wave-front distortion (which includes piston) and a variance reduction factor that removes the piston:

$$\sigma^2_{\phi,eff} = \sigma^2_{\phi,\infty}\, vrf \tag{20}$$

The variance reduction factor is obtained by dividing the effective phase variance of Eq. (11) by the phase variance of Eq. (12). For beacons that can be characterized by one size parameter, say d, the variance reduction factor can be written in terms of an auxiliary function, K(e), called the non-piston fraction, that depends on the beacon geometry:

$$vrf = \int_0^1 d\gamma\gamma^{5/3}C_n^2(\gamma L)K\left(R\hat{\gamma}/(\gamma d)\right)\Big/\int_0^1 d\gamma\gamma^{5/3}C_n^2(\gamma L) \tag{21}$$

8

The turbulence is assumed to be isotropic. For the offset point beacon geometry, the non-piston fraction is given by

$$K^{OP}(e) = 0.4471\int_0^\infty d\mu\mu^{-8/3}\left[1-\Lambda_1^2(\mu e)\right]2(1-J_0(\mu)) \tag{22}$$

and the beacon size parameter d in Eq. (21) is the beacon offset, b_o. A numerical evaluation of the offset point beacon non-piston fraction is shown in Fig. 3. The numerical integration of Eq. (22) is performed with the following techniques. For very small values of μ, the integrand is expanded into a power series (up to eighth order in μ), and the terms are integrated separately and added. The Bessel function terms are divided into two pieces. The first piece extends over about five oscillations, where the Bessel function itself is used. The second piece extends from the end of the first piece to infinity, and applies an exponential damping to the Bessel function oscillations. The integral can be truncated at some value of μ because of the inverse weighting in the integrand. For a given value of e, the quadrature is successively reduced until further improvement is sufficiently small (five significant figures). The upper limit of the integration is also extended until further contributions are negligible.

For an on-axis uniform circular beacon, the non-piston fraction is found to be

$$K^{UC}(e) = 6.4508\int d\mu\mu^{-8/3}\left[1-\Lambda_1^2(\mu e)\right](1-\Lambda_1(\mu)) \tag{23}$$

and the beacon size parameter d in Eq. (21) is the beacon radius, R_b. The non-piston fraction for the uniform circular beacon is also shown in Fig. 3.

To find the anisoplanatic phase variance in a particular application, the appropriate non-piston fraction and the expected turbulence profile are used to obtain the variance reduction factor. This will generally require numerical integration with a given specific turbulence profile. The dependence on the turbulence profile will be assessed by treating two extreme idealized profiles: uniform along the path, and highly localized turbulence.

For a uniform turbulence profile, the variance reduction factor of Eq. (21) simplifies to

$$vrf_{uniform} = \frac{8}{3}\int_0^1 d\gamma\gamma^{5/3}K\left(\frac{R\hat{\gamma}}{d\gamma}\right) \tag{24}$$

A normalized aperture diameter can be defined in terms of the atmospheric coherence length and the mean square wave-front distortion

$$\hat{D} = \frac{D}{r_0\left(\sigma^2_{\varphi,\infty}\right)^{3/5}} \tag{25}$$

or in terms of the isoplanatic patch and beacon size $\hat{D}_{OP} = \frac{D}{r_0}\frac{L\theta_0}{b_0}$ and $\hat{D}_{UC} = \frac{D}{r_0}\frac{L\theta_0}{0.2016b_0}$.

For the uniform turbulence profile, the atmospheric coherence length and the isoplanatic angle are related by $L\theta_0 / r_0 = 0.3144$. The finite aperture variance reduction factors for a uniform turbulence profile can then be expressed as functions of the normalized aperture diameter:

$$vrf^{OP}_{uniform} = \tfrac{8}{3}\int_0^1 d\gamma\gamma^{5/3}K^{OP}(1.590\hat{D}(1-\gamma)/\gamma) \tag{26}$$

9

$$vrf_{uniform}^{UC} = \tfrac{8}{3}\int_0^1 d\gamma\gamma^{5/3}\, K^{UC}(0.3206\hat{D}(1-\gamma)/\gamma)$$

These variance reduction factors are shown in Fig. 4.

The Dirac turbulence profile, i.e. $C_n^2(\gamma L) = \delta(\gamma - \gamma_0)\Delta C_{no}^2$, can be used to characterize the variance reduction for cases where the turbulence is highly localized. This corresponds to a region of turbulence located at a distance γ_oL from the aperture, spread over a distance Δ, and having strength C_{no}^2. In this case, the variance reduction factor of Eq. (21) simplifies to

$$vrf_{Dirac} = K\left(\frac{R\hat{\gamma}_0}{d\gamma_0}\right) \tag{27}$$

Any ratio of coherence length to isoplanatic patch can be approximated, depending on the location of the turbulence in the path: $L\theta_0 / r_0 = 0.3144(1-\gamma_0)/\gamma_0$. The variance reduction factors for the Dirac profile with the offset point and the uniform circular beacons are then

$$\begin{aligned} vrf_{Dirac}^{OP} &= K^{OP}(1.590\hat{D}_{OP}) \\ vrf_{Dirac}^{UC} &= K^{UC}(0.3206\hat{D}_{UC}) \end{aligned} \tag{28}$$

These finite aperture variance reduction factors for localized turbulence profiles are shown in Fig. 5.

When the normalized aperture is large, the asymptotic variance reduction factor is unity. However, the large aperture asymptotic value is reached at a smaller normalized aperture for the uniform circular beacon than for the offset point beacon. This indicates that the residual phase variance with the uniform circular beacon has a much smaller contribution from low order modes (in particular, piston) than does the offset point beacon.

In the small normalized aperture limit, regardless of the turbulence profile, asymptotic behavior of the variance reduction factors is found to be

$$\begin{aligned} \lim_{\hat{D}_{OP}\to 0} vrf^{OP} &= 2.066\hat{D}_{OP}^{5/3} \\ \lim_{\hat{D}_{UC}\to 0} vrf^{UC} &= 1.033\hat{D}_{UC}^{5/3} \end{aligned} \tag{29}$$

These asymptotic values combine with Eq. (20) to give the phase variance when the beacon size (normalized to the isoplanatic patch) is large relative to the aperture (normalized to the coherence length). For the offset point beacon, the phase variance in this limit is exactly twice the phase variance for uncompensated turbulence. When the offset is sufficiently large, the phase error sensed by the beacon is uncorrelated to the required phase correction of the outgoing beam, so that the total variance is the sum of the beacon and outgoing beam variances, i.e. twice the uncompensated result. For the uniform circular beacon in this limit, the phase variance approaches the uncompensated value, rather than twice the uncompensated value, because for a large uniform beacon, the sampled phase variance will average to zero.

10

SUMMARY

A methodology has been laid out by which the anisoplanatic effects of distributed beacon sources can be evaluated for focused beam geometries. Its application is in determining the performance limitations of an adaptive optics wavefront compensation system, where the wavefront sensor uses the return from an illuminated target. For any beacon source intensity distribution, Eq. (10) is used to find the appropriate anisoplanatic filter. This filter is then used as a weighting function for the integration over the turbulence spectrum. Eq. (11) then gives the integral that must be performed over the turbulence profile to obtain the residual anisoplanatic phase variance. This phase variance is then used to obtain the Strehl ratio for the compensated beam. A number of practical beacon distributions have been treated analytically, and two extreme turbulence profiles have been employed, to illuminate trends.

The key result is that the spread of the beacon distribution has much less deleterious effect than the offset of the beacon centroid from the aimpoint. It was also seen that some anisoplanatic effects with collimated beam geometry are qualitatively different from those in a focused beam geometry.

11

REFERENCES

1. F. Merkle, and J. M. Beckers, “Application of adaptive optics to astronomy,” Proc. SPIE (Int. Soc. Opt. Eng.) **1114**, 2 (1989).
2. C. S. Gardner, B. M. Welsh, L. A. Thompson, “Design and performance analysis of adaptive optical telescopes using laser guide stars,” Proc. IEEE **78**, 1721-1743 (1990).
3. B. G. Zollars, “Atmospheric-turbulence compensation experiments using synthetic beacons,” MIT Lincoln Laboratory Journal **5**, 67-92 (1992).
4. D. V. Murphy, “Atmospheric-turbulence compensation experiments using cooperative beacons,” MIT Lincoln Laboratory Journal **5**, 25-44 (1992).
5. D. L. Fried, “Anisoplanatism in adaptive optics,” J.Opt.Soc.Am. **72**, 52-61 (1982).
6. R. J. Sasiela, “Strehl ratios with various types of anisoplanatism,” J. Opt. Soc. Am. A 9, 1398-1405 (1992).
7. H. T. Yura, and S. G. Hanson, “Second-order statistics for wave propagation through complex optical systems,” J. Opt. Soc. Am. A 6, 564-575 (1989).
8. R. J. Sasiela, "A Unified Approach to Electromagnetic Wave Propagation in Turbulence and the Evaluation of Multiparameter Integrals,” Rep. TR-807 ADA 198062 (Lincoln Laboratory , Massachusetts Institute of Technology, Lexington, Mass., 1988).
9. G. A. Tyler, “Rapid evaluation of do: the effective diameter of a laser-guide-star adaptive-optics system,” J. Opt. Soc. Am. A **11**, 325-338 (1994).
10. D. L. Fried, and J. F. Belsher, “Analysis of fundamental limits to artificial-guide-star adaptive-optics-system performance for astronomical imaging,” J. Opt. Soc. Am. A **11**, 277-287 (1994).
11 B. M. Welsh, and C. S. Gardner, “Effects of turbulence-induced anisoplanatism on the imaging performance of adaptive-astronomical telescopes using laser guide stars,” J. Opt. Soc. Am. A **8**, 69-80 (1991).
12. G. A. Tyler, “Wave-front compensation for imaging with off-axis guide stars,” J. Opt. Soc. Am. A **11**, 339-346 (1994).
13. J. Stone, P. H. Hu, S. P. Mills, S. Ma, “Anisoplanatic effects in finite-aperture optical systems,” J. Opt. Soc. Am. A **11**, 325-338 (1994).
14. R. J. Sasiela, “Wave-front correction by one or more synthetic beacons,” J. Opt. Soc. Am. A **11**, 379-393 (1994).
15. M. Born, and E. Wolf, Principles of Optics, sixth (corrected) edition, Pergamon Press, Oxford (1980).
16. G. A. Tyler, “Turbulence-induced adaptive-optics performance degradation: evaluation in the time domain,” J. Opt. Soc. Am. A **1**, 251-262 (1984).
17. H. T. Yura, “An elementary derivation of phase fluctuations of an optical wave in the atmosphere,” Proc. SPIE (Int. Soc. Opt. Eng.) **75**, 9-15 (1976).
18. R. G. Frehlich, “Variance of focal-plane centroids,” J. Opt. Soc. Am. A **7**, 2119-2140 (1990).
19. R. R. Butts, and C. B. Hogge,” Phase conjugate adaptive optics using perimeter phase measurement,” J. Opt. Soc. Am. **67**, 278-281 (1977).
20. R. J. Noll, “Zernike polynomials and atmospheric turbulence,” J. Opt. Soc. Am. **66**, 207-211 (1976).
21. V. I. Tatarski, “Wave Propagation in a Turbulent Medium," McGraw-Hill Book Co. (1961).
22. M. Abramowitz, and I. Stegun, ”Handbook of Mathematical Functions,” Dover, NY (1965).

12

23. I. S. Gradshteyn, and I. M. Ryzhik, “Table of integrals, series, and products,” Academic Press, inc., Orlando (1980).

13

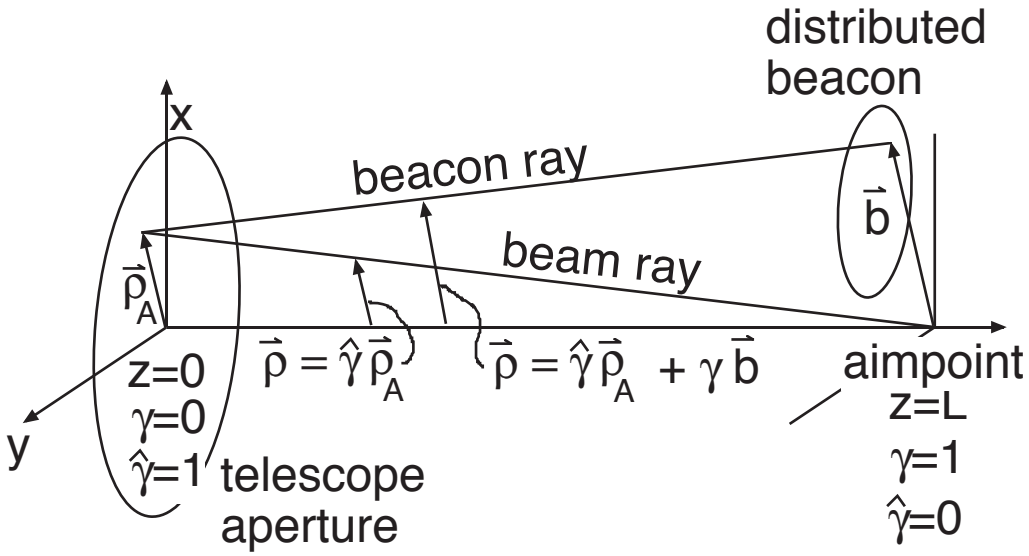

Fig. 1. The geometry and nomenclature for treating a focused beam and a distributed beacon.

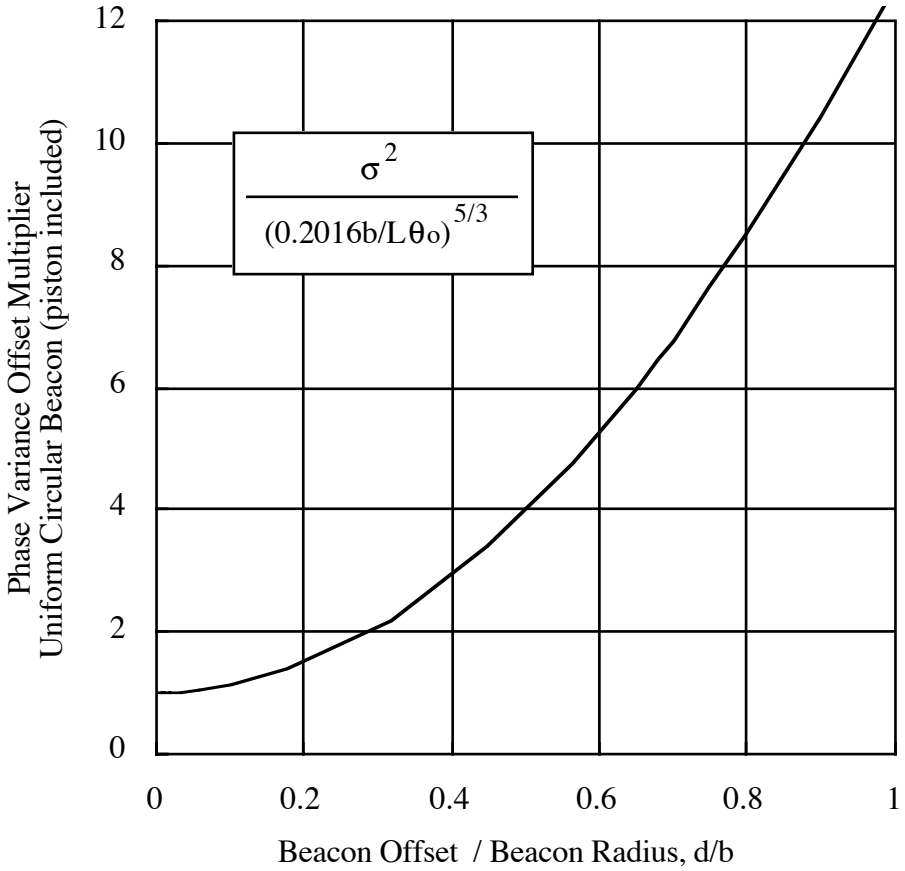

Fig. 2. The anisoplanatic phase variance multiplier, that accounts for the mean square wave-front distortion increase due to offset of the centroid by a distance d from the aimpoint, of a uniform circular beacon of radius b.

14

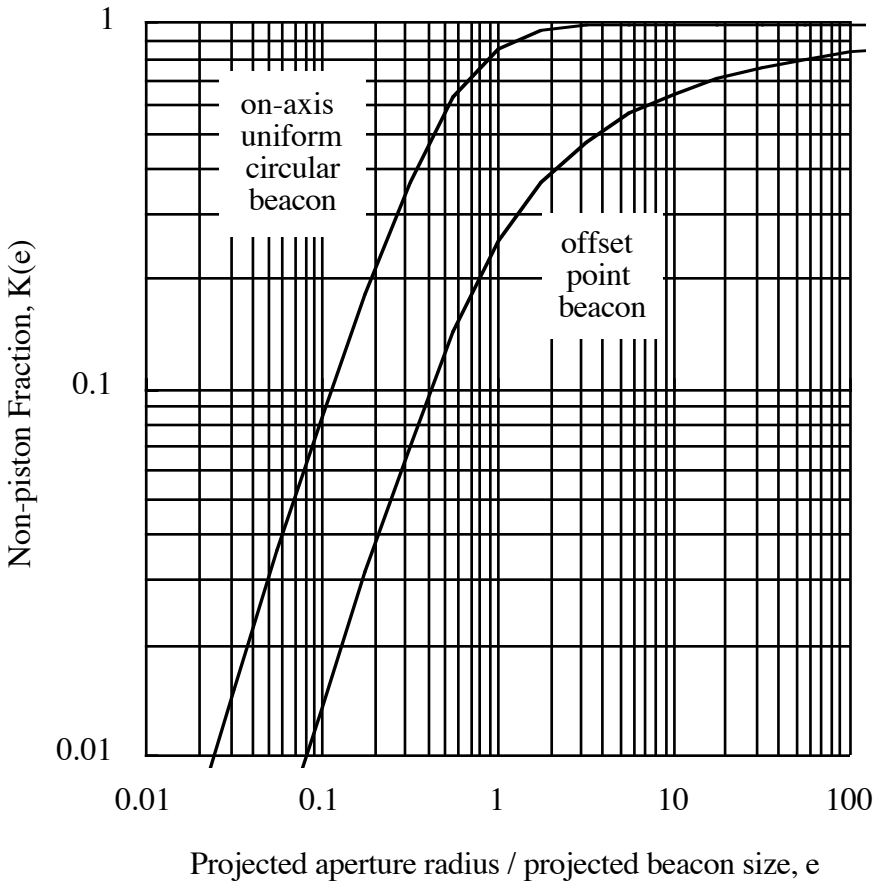

Fig. 3. The non-piston fraction, as a function of the ratio of the projected beacon offset to the projected beacon radius.

15

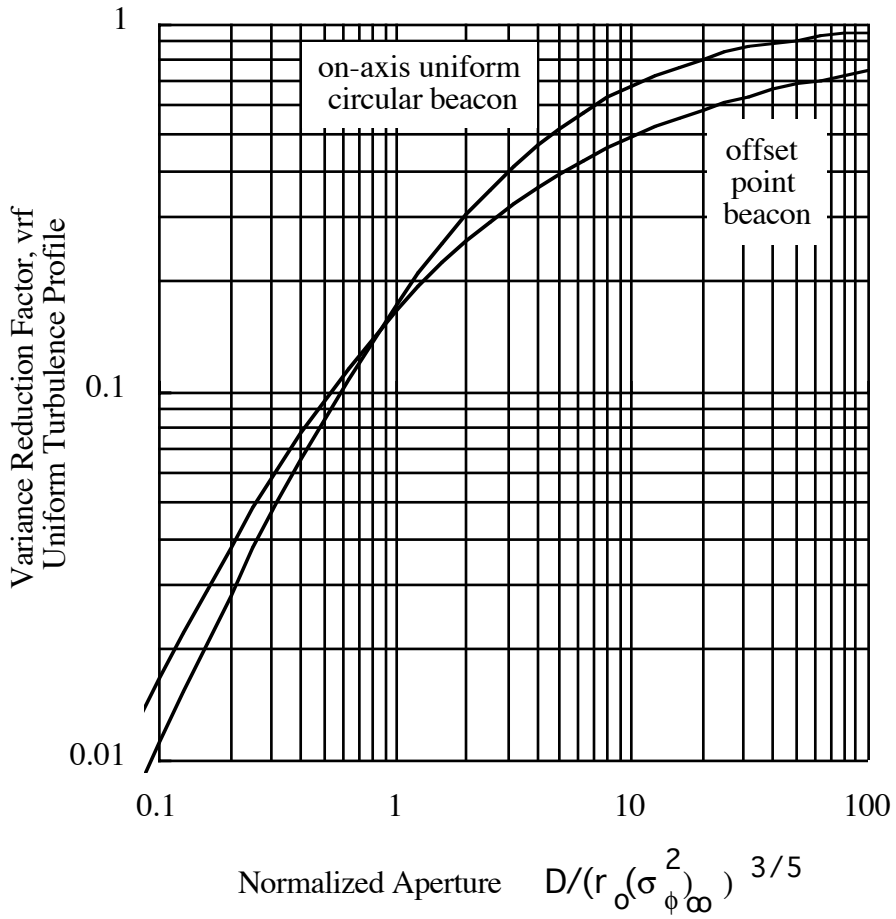

Fig. 4. The variance reduction factor due to finite aperture for a uniform turbulence profile. The aperture is normalized with the atmospheric coherence length and the mean square wave-front distortion.

16

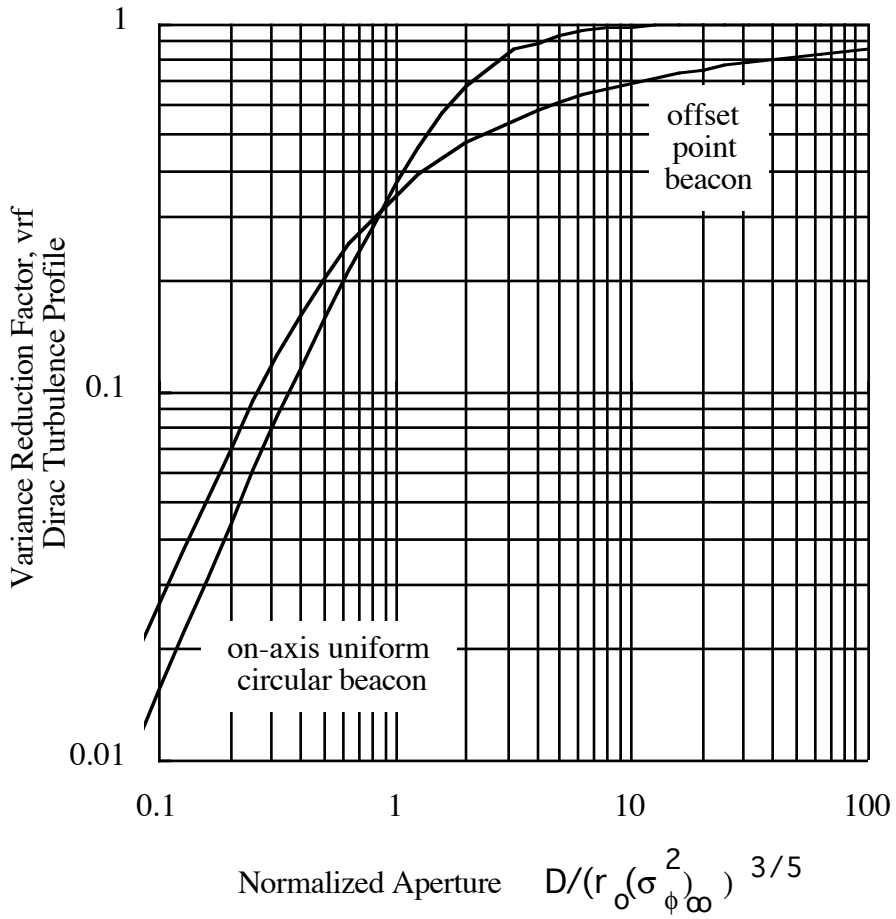

Fig. 5. The variance reduction factor due to finite aperture for a highly localized turbulence profile. The aperture is normalized with the atmospheric coherence length and the mean square wave-front distortion.

17